

REPORT DOCUMENTATION PAGE				Form Approved OMB NO. 0704-0188	
<p>The public reporting burden for this collection of information is estimated to average 1 hour per response, including the time for reviewing instructions, searching existing data sources, gathering and maintaining the data needed, and completing and reviewing the collection of information. Send comments regarding this burden estimate or any other aspect of this collection of information, including suggestions for reducing this burden, to Washington Headquarters Services, Directorate for Information Operations and Reports, 1215 Jefferson Davis Highway, Suite 1204, Arlington VA, 22202-4302. Respondents should be aware that notwithstanding any other provision of law, no person shall be subject to any penalty for failing to comply with a collection of information if it does not display a currently valid OMB control number.</p> <p>PLEASE DO NOT RETURN YOUR FORM TO THE ABOVE ADDRESS.</p>					
1. REPORT DATE (DD-MM-YYYY) 29-07-2012		2. REPORT TYPE Final Report		3. DATES COVERED (From - To) 1-Jun-2008 - 31-May-2012	
4. TITLE AND SUBTITLE Flame Propagation and Blowout in Hydrocarbon Jets: Experiments to Understand the Stability and Structure				5a. CONTRACT NUMBER W911NF-08-1-0142	
				5b. GRANT NUMBER	
				5c. PROGRAM ELEMENT NUMBER 611102	
6. AUTHORS Kevin M. Lyons				5d. PROJECT NUMBER	
				5e. TASK NUMBER	
				5f. WORK UNIT NUMBER	
7. PERFORMING ORGANIZATION NAMES AND ADDRESSES North Carolina State University Office of Contract and Grants Leazar Hall Lower Level- MC Raleigh, NC 27695 -7214				8. PERFORMING ORGANIZATION REPORT NUMBER	
9. SPONSORING/MONITORING AGENCY NAME(S) AND ADDRESS(ES) U.S. Army Research Office P.O. Box 12211 Research Triangle Park, NC 27709-2211				10. SPONSOR/MONITOR'S ACRONYM(S) ARO	
				11. SPONSOR/MONITOR'S REPORT NUMBER(S) 53429-EG.18	
12. DISTRIBUTION AVAILABILITY STATEMENT Approved for Public Release; Distribution Unlimited					
13. SUPPLEMENTARY NOTES The views, opinions and/or findings contained in this report are those of the author(s) and should not be construed as an official Department of the Army position, policy or decision, unless so designated by other documentation.					
14. ABSTRACT This research supported by the U.S. Army Research Office examines a myriad of facets of lifted hydrocarbon jet flames in the presence of air co-flow. At a certain jet exit velocity, a flame will lift from the fuel nozzle and stabilize at some downstream position. The partially-premixed flame front of the lifted flame oscillates, with the oscillations becoming greater in flames stabilized further downstream. These					
15. SUBJECT TERMS Combustion, Turbulent Reacting Flows, Flame Stabilization, Jet Flow, Experimental Fluids					
16. SECURITY CLASSIFICATION OF:			17. LIMITATION OF ABSTRACT UU	15. NUMBER OF PAGES	19a. NAME OF RESPONSIBLE PERSON Kevin Lyons
a. REPORT UU	b. ABSTRACT UU	c. THIS PAGE UU			19b. TELEPHONE NUMBER 919-515-5293

## Report Title

Flame Propagation and Blowout in Hydrocarbon Jets:  
Experiments to Understand the Stability and Structure

### ABSTRACT

This research supported by the U.S. Army Research Office examines a myriad of facets of lifted hydrocarbon jet flames in the presence of air co-flow. At a certain jet exit velocity, a flame will lift from the fuel nozzle and stabilize at some downstream position. The partially-premixed flame front of the lifted flame oscillates, with the oscillations becoming greater in flames stabilized further downstream. These oscillations are also observed in flames where blowout is imminent. Research progress has been made in a) flame blowout in diluted jets and confined co-flow systems, b) flame hysteresis in diluted and confined jets, c) reacting jets in air cross-flows to examine the nature of the stability characteristics and d) electrostatic flow control, that has potential for combustion control applications. The research has involved both undergraduate and graduate students, and has been published in the literature.

---

**Enter List of papers submitted or published that acknowledge ARO support from the start of the project to the date of this printing. List the papers, including journal references, in the following categories:**

#### (a) Papers published in peer-reviewed journals (N/A for none)

<u>Received</u>	<u>Paper</u>
2011/06/27 11 13	Wei Wang, Kevin M. Lyons. Leading-Edge Velocities and Lifted Methane Jet Flame Stability, Journal of Combustion, (01 2010): . doi:
2011/06/27 11 12	Nancy J. Moore, James Kribs, Kevin M. Lyons. Investigation of Jet-Flame Blowout with Lean-Limit Considerations, Flow, Turbulence and Combustion, (03 2011): . doi:
2011/06/27 11 11	NJ Moore and KM Lyons. Leading-Edge Flame Fluctuations in Lifted Turbulent Flames, Combustion Science and Technology, (07 2010): . doi:
2011/06/27 11 10	K. M. Lyons, N. J. Moore, J. L. McCraw, K. A. Watson, C. D. Carter, J. M. Donbar. On Flame-Edge Propagation, Flow, Turbulence and Combustion, (02 2008): . doi:
2011/06/27 11 8	Michael S. June*, James Kribs, Kevin M. Lyons. Efficiency of electrostatic air moving devices, Journal of Electrostatics, (06 2010): . doi:
2010/01/07 11 4	N. J. Moore, J. L. McCraw, and K. M. Lyons. Observations on Jet Flame Blowout, , (01 2010): . doi:

**TOTAL: 6**

**Number of Papers published in peer-reviewed journals:**

---

#### (b) Papers published in non-peer-reviewed journals (N/A for none)

<u>Received</u>	<u>Paper</u>
2012/07/04 11 17	Nancy Moore, Steve Terry, Kevin Lyons. Flame Hysteresis Effects in Methane Jet Flames in Air-Coflow, Journal of Energy Resources Technology, (06 2011): 202. doi:
2011/06/27 11 9	Michael S. June*, James Kribs, Kevin M. Lyons. Measuring efficiency of positive and negative ionic wind devices for comparison to fans and blowers, Journal of Electrostatics, (05 2011): . doi:
2010/01/07 11 2	David A. Wilson and Kevin M. Lyons. On Diluted-Fuel Combustion Issues in Burning Biogas Surrogates, ASME-JERT, (12 2009): . doi:

**TOTAL: 3**

**Number of Papers published in non peer-reviewed journals:**

---

**(c) Presentations**

The Effects of Collector Surface Area with Electrostatic Flows Resulting from Multiple Corona Discharges” Michael S. June, James Kribs and Kevin M. Lyons, IEEE Pulsed Power Conference, Washington DC, June 2009.

“Utilizing Multiple Corona Discharges as an Ionic Air Moving Device” Kribs J.1, June M.1, Lyons K. Interdisciplinary Conference on Chemical, Mechanical and Materials Engineering (2009 ICCMME) Australian Institute of High Energetic Materials, Melbourne, Australia December 2009.

“Development of Thermal Manikin Hands for Characterizing the Thermal Protective Performance of Gloves in Flash Fire Exposures”, A.C. Hummel, R.L. Barker, K.M. Lyons, A.S. Deaton and J.J. Morton-Aslanis, 2010 AATCC International Conference - Innovative Technologies, Atlanta, May 2010.

**Number of Presentations:** 3.00

---

**Non Peer-Reviewed Conference Proceeding publications (other than abstracts):**

<u>Received</u>	<u>Paper</u>
-----------------	--------------

**TOTAL:**

**Number of Non Peer-Reviewed Conference Proceeding publications (other than abstracts):**

---

**Peer-Reviewed Conference Proceeding publications (other than abstracts):**

<u>Received</u>	<u>Paper</u>
2012/07/04 1' 16	Tamir Hasan, James Kribs, Kevin Lyons. INFLUENCES OF NITROGEN DILUTION IN THE NEAR FLOW FIELD OF TRANSITION REGIME LIFTED NATURAL GAS JET FLAMES, ASME 2011 International Mechanical Engineering Congress & Exposition. 2011/11/11 00:00:00, . : ,
2012/07/04 1' 15	James Kribs, Tamir Hasan, Kevin Lyons. NITROGEN DILUTED JET FLAMES IN THE PRESENCE OF COFLOWING AIR, ASME 2011 International Mechanical Engineering Congress & Exposition. 2011/11/11 00:00:00, . : ,

**TOTAL: 2**

**Number of Peer-Reviewed Conference Proceeding publications (other than abstracts):**

---

**(d) Manuscripts**

<u>Received</u>	<u>Paper</u>
2011/06/27 1' 6	N. J. Moore, S. D. Terry and K. M. Lyons. Flame Hysteresis Effects in Methane Jet Flames in Air-Coflow, (06 2011)
2010/01/07 1' 3	N. J. Moore and K. M. Lyons. Leading-Edge Flame Fluctuations in Lifted Turbulent Flames , Combustion Science and Technology (01 2010)

**TOTAL: 2**

**Number of Manuscripts:**

---

**Books**

TOTAL:

Patents Submitted

Patents Awarded

Awards

Graduate Students

<u>NAME</u>	<u>PERCENT SUPPORTED</u>	Discipline
Nancy Moore	0.25	
Wei Wang	0.10	
James Kribs	0.50	
Sean June	0.05	
Jen McCraw	0.05	
<b>FTE Equivalent:</b>	<b>0.95</b>	
<b>Total Number:</b>	<b>5</b>	

Names of Post Doctorates

<u>NAME</u>	<u>PERCENT SUPPORTED</u>
<b>FTE Equivalent:</b>	
<b>Total Number:</b>	

Names of Faculty Supported

<u>NAME</u>	<u>PERCENT SUPPORTED</u>	National Academy Member
Kevin Lyons	0.10	
<b>FTE Equivalent:</b>	<b>0.10</b>	
<b>Total Number:</b>	<b>1</b>	

Names of Under Graduate students supported

<u>NAME</u>	<u>PERCENT SUPPORTED</u>	Discipline
Tamir Hasan	0.10	Mechanical Engineering
<b>FTE Equivalent:</b>	<b>0.10</b>	
<b>Total Number:</b>	<b>1</b>	

### Student Metrics

This section only applies to graduating undergraduates supported by this agreement in this reporting period

The number of undergraduates funded by this agreement who graduated during this period: .....

The number of undergraduates funded by this agreement who graduated during this period with a degree in science, mathematics, engineering, or technology fields:.....

The number of undergraduates funded by your agreement who graduated during this period and will continue to pursue a graduate or Ph.D. degree in science, mathematics, engineering, or technology fields:.....

Number of graduating undergraduates who achieved a 3.5 GPA to 4.0 (4.0 max scale): .....

Number of graduating undergraduates funded by a DoD funded Center of Excellence grant for Education, Research and Engineering: .....

The number of undergraduates funded by your agreement who graduated during this period and intend to work for the Department of Defense .....

The number of undergraduates funded by your agreement who graduated during this period and will receive scholarships or fellowships for further studies in science, mathematics, engineering or technology fields: .....

### Names of Personnel receiving masters degrees

NAME

Jon Gomes

**Total Number:** 1

### Names of personnel receiving PhDs

NAME

Nancy Moore

Sean June

**Total Number:** 2

### Names of other research staff

NAME

PERCENT SUPPORTED

**FTE Equivalent:**

**Total Number:**

### Sub Contractors (DD882)

### Inventions (DD882)

## **Scientific Progress**

The main advances in jet flame flow interaction in oblique jet/air flows, as well as flame blowout, are detailed in the attachment.

## **Technology Transfer**

Prepared for the U.S. Army Research Office

Supported by ARO Grant/Contract Number: W911NF-08-1-0142

Technical Accomplishment Description for the Final Report of

FLAME PROPAGATION AND BLOWOUT IN HYDROCARBON JETS: EXPERIMENTS  
TO UNDERSTAND THE STABILITY AND STRUCTURE OF REACTION ZONES

PI: Kevin M. Lyons

North Carolina State University

## Part A) Advances on the Stability and Blowout Behavior of Jet Flames in Oblique Air Flows

### ABSTRACT

The stability limits of a jet flame can play an important role in the design of burners and combustors. This study details an experiment conducted to determine the liftoff and blowout velocities of oblique-angle methane jet flames under various air coflow velocities. A nozzle was mounted on a telescoping boom to allow for an adjustable burner angle relative to a vertical coflow. Twenty-four flow configurations were established using six burner nozzle angles and four coflow velocities. Measurements of the fuel supply velocity during liftoff and blowout were compared against two parameters: nozzle angle and coflow velocity. The resulting correlations indicated that flames at more oblique angles have a greater upper stability limit and were more resistant to changes in coflow velocity. This behavior occurs due to a lower effective coflow velocity at angles more oblique to the coflow direction. Additionally, stability limits were determined for flames in crossflow and mild counterflow configurations, and a relationship between the liftoff and blowout velocities was observed. For flames in crossflow and counterflow, the stability limits are higher. Further studies may include more angle and coflow combinations, as well as the effect of diluents or different fuel types.



## **1. Introduction**

A multitude of studies have been performed on lifted jet flames and their behavior in various air flow configurations. In such partially-premixed flames, the characteristics of the surrounding air flow (velocity, temperature) can strongly impact the overall combustion process and the stability parameters. As fuel flows from a nozzle and mixes with the air, the fuel and oxidizer concentrations vary throughout space and time. The extent of mixing due to turbulence also changes depending on the surrounding flow. The perpetually varying concentrations help to determine the overall behavior of a flame: its shape, velocity, size, color, temperature, and composition. In parallel, the heat release serves to laminarize regions, and serves to limit reducing mixing.

In particular, two important behavioral parameters are liftoff and blowout velocity. Initially, a jet flame will remain attached to the nozzle at low fuel velocities. However, at a critical jet velocity, the flame will lift off from the nozzle and stabilize at a position downstream due to the inability of the flame to remain anchored on the burner [1]. While there is, in general, a regime where the flame can stabilize, increasing the jet velocity will ultimately lead to blowout, in which the flame is extinguished. This behavior occurs at some critical blowout velocity. Together, the liftoff and blowout velocities essentially define the stability limits of a lifted jet flame.

Typically, past experiments on liftoff and blowout have focused on coaxial flow. In this arrangement, the jet nozzle is parallel to a surrounding airflow (coflow). Another common arrangement is transverse flow, in which the nozzle is perpendicular to the airflow

(crossflow). Jet diffusion flames behave differently in both arrangements, as previously performed experiments have demonstrated.

Early major experiments involving flame stability in coflow were conducted by Wohl et al around 1950 [2]. They determined that the liftoff and blowout velocities (stability limits) are functions of the supply (jet) velocity and fuel concentration. When the supply velocity is less than the flame velocity, then the flame will flash back into the burner. In contrast, the flame will lift off from the burner and equilibrate downstream when the supply velocity exceeds a critical value. Later, Vanquickenbourne and van Tiggelen [3] expanded on Wohl by suggesting that the liftoff height occurs where the mean incoming fuel velocity equals the turbulent burning velocity of the flame (induced under coflow). Their work has served as the foundation for other experiments involving the modeling of jet diffusion flames.

Another major development occurred in 1984 with the work of Kalghatgi [4], who built on the previous work of Vanquickenbourne and Tiggelen. He observed that the flame liftoff height for hydrogen, propane, methane, and ethylene depends on several physical parameters—and strongly on the jet exit velocity. A linear correlation exists between the two variables, regardless of the burner diameter. After performing a nondimensional analysis of his data, Kalghatgi concluded that diffusion flames blow out at a height that is 0.65-0.75 times the height of the stoichiometric contour. According to his findings, the height is also inversely proportional to the square of the laminar burning velocity.

Brown et al have studied the effect of jet exit velocity and coflow velocity on liftoff height [5]. They discovered that the former has a minimal effect on lifted flames that are significantly downstream from the burner exit (i.e., in the far field). In this area, the turbulent

burning velocity equals the flame stabilization velocity. However, in the near field relative to the burner, findings reveal that the stabilization velocity is approximately equal to three times the laminar burning velocity.

The work of Vanquickenbourne and van Tiggelen also formed the basis for a study by Tieszen et al which explored blowout mechanisms [6]. Their results confirmed the theory proposed by Vanquickenbourne and van Tiggelen: blowout occurs when the local flow velocity exceeds the turbulent burning speed of the flame. However, they also investigated the role of large-scale eddies, concluding that they are responsible for flame propagation in the interior of the jet. Burgess and Lawn [7] have expanded on the work of Vanquickenbourne and van Tiggelen by including the effects of large eddy structures and locations where the flame is relatively stable. Imaging and direct numerical simulations revealed that flames tend to propagate near large eddies, but away from the center where the mixture is too rich. In addition, Navarro-Martinez and Kronenburg [8] have consolidated results from large eddy simulations (LES) for multiple lifted flame configurations. They assert that the conditional moment closure approach can accurately predict stability conditions based on experimental behavior. Recently, more studies have focused on modeling and simulating jet flames using LES and other techniques.

While jet behavior in coflow has been extensively studied, less attention has been devoted to jets in crossflow. In a review, Bandaru and Turns included a comprehensive list of all major crossflow research to date [9]. Many of the works relevant to this study were observation-based experiments performed by Kalghatgi, whose crossflow flame experiments were conducted in a wind tunnel and involved propane, methane, and ethylene fuels. In

parallel with the research on flame liftoff height in coflow, Kalghatgi investigated flames in a cross-wind normal to the burner axis [10]. His findings revealed two distinct blowout limits for flames in a moderate cross-wind: a lower limit in which the incident wind extinguishes the flame and an upper limit in which the flame blows itself out. At the lower limit, the jet velocity is much lower than the blowout velocity of a jet in still air. However, at the upper limit, the blowout mechanism is similar to that of a flame in still air. The upper blowout limit is usually greater than the blowout velocity in still air due to greater levels of turbulence caused by the cross-wind. Kalghatgi's experimental results demonstrated that a lifted, stable flame can exist between the upper and lower blowout limits.

Kalghatgi also investigated the effect of burner orientation to wind direction [11]. Burner diameters ranged from 4 mm to 20 mm, while the angle between the wind direction and burner axis varied between  $45^\circ$ ,  $66^\circ$ ,  $90^\circ$ ,  $114^\circ$ , and  $135^\circ$ . By measuring the jet velocity at which blowout occurs (at the lower limit), Kalghatgi concluded that jet flames are less prone to blowout as the burner angle increases from  $0^\circ$  to  $180^\circ$ . He also discovered that the lower blowout limit does not always exist under low wind speeds. In such conditions, a flame will stabilize in the wake of the burner and the wind cannot extinguish it, especially at angles greater than  $90^\circ$ . Thus, flame behavior is difficult to predict in these conditions.

In another study, Han and Mungal observed the mixing and combustion processes of jet flames injected at  $-45^\circ$ ,  $0^\circ$ , and  $45^\circ$  [12]. Using particle image velocimetry (PIV) and CH PLIF imaging techniques, they concluded that flame length increases with injection angle due to reduced entrainment. They also attempted to model the dilation behavior of the stoichiometric contour, which they suggest occurs due to the premixed characteristics of

deflected jet flames. Hasselbrink and Mungal performed a similar study in which the velocity fields of transverse ( $0^\circ$ ) jet flames was measured using PIV [13]. Overall, they noted greater flame/flow interaction near the base of the lifted flame than at downstream locations.

The purpose of this experiment is to delineate flame stability and blowout behavior at several oblique angles under various flow velocity ratios. Despite a much smaller scale, understanding the behavior of angled flames in an experimental setting can aid in the proper design of flaring towers and burners that account for varying wind conditions, as well as assess conditions in low-turndown industrial burners. By consolidating the overall results, an optimal burner configuration may be chosen based on desired stability and blowout parameters, as well as a relationship between the flame liftoff velocity and blowout.

## 2.) Experimental Arrangement

The apparatus used for angled jet experiments is shown in Figure 1. This apparatus was used for previous experiments involving flame stability behavior in coflow and has been described in detail in earlier publications [14] [15].

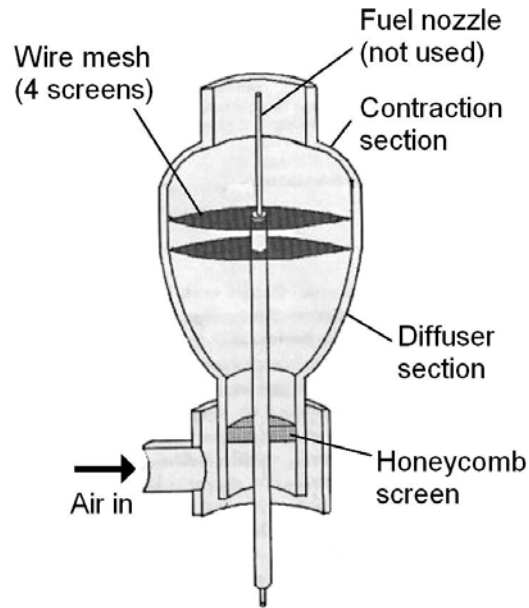


**Figure 1. Burner apparatus for angled jet experiments.**

The fuel tube consists of a 3 mm fuel nozzle that is concentric with a large annulus for air coflow (6 inch). However, this nozzle was not used for angled jet flames. Instead, an appropriate nozzle was devised from 0.25" (6.35 mm) stainless steel tubing mounted on a telescoping boom with an adjustable angle, as shown in Fig. 2. To determine the angle of the nozzle, a protractor was mounted on the boom. Using a string with a weight at the end (which provided a vertical line of reference), the angle could be read off the protractor. The nozzle is oriented such that it is in the uniform velocity region of the coflow, away from the edges. A vertical distance of 11 inches is maintained between the nozzle and the top of the burner to avoid any irregularities in the air coflow.

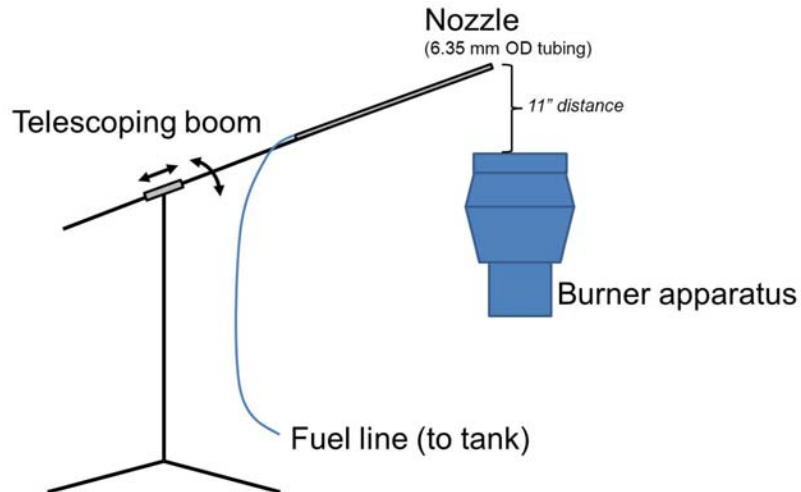


**Figure 2. Nozzle on telescoping boom**

The coflow air is pumped by a Magnetek model 9467 centrifugal blower, controlled with a potentiometer to allow for variable operation speeds. The coflow then travels through flexible hose (5 inches in diameter) to the burner. The air travels through a 90° tee before entering a 2.54-mm thick honeycomb screen. The screen makes the coflow velocity profile more uniform and straight. After the screen, the coflow air enters a diffuser section with a greater cross-section area. The diffuser section contains four wire mesh screens which serve to eliminate flow irregularities and further refine the coflow velocity profile into a “top-hat” shape. Finally, the coflow air exits the burner through a contraction section with a terminating diameter of 150 mm.

The coflow air velocity is measured using a TSI Veloci-calc model 8345 hot-wire anemometer, which displayed values in meters per second with a precision of 0.01 m/s and an accuracy of  $\pm 3\%$  of the reading. For each coflow velocity measurement, the tip of the wand (containing the sensing element) is placed horizontally on the burner exit, perpendicular to the coflow direction. The potentiometer controlling the blower motor is then

adjusted to achieve the desired coflow velocities of 0, 0.25, 0.40, and 0.60 m/s. With the coflow direction constrained to a vertical, upwards flow, it was necessary to adjust the direction of the fuel jet, and this adjustment changed the direction of other forces, such as natural buoyancy. This setup is similar to previous work in oblique flows done by G.T. Kalghatgi, by having the coflowing air act in one direction, but varying the angle, at which the fuel jet flows [11]. With the limitation of the size of the coflowing air region, the location of the nozzle and the flame base were important factors. The jet nozzle was maintained at the center of the coflow ring, in order to keep the flame base within the coflow region, which was the main area of interest, as it is the focus of flame stabilization.

The fuel volumetric flow rate is measured using an Advance Series 150 flowmeter, calibrated for use with methane. The flowmeter consists of a stainless steel ball in a graduated cylinder. Readings are taken from the bottom of the ball and converted into units of scfh (standard cubic feet per hour) using the manufacturer's charts. The jet velocity can then be calculated based on the volumetric flow rate and cross-sectional area of the burner. The gas is supplied from a pressurized cylindrical tank and regulated through a MicroLine UHP Gas Panel controller. The speed of the coflowing air was set, as was the angle of nozzle, with regards to the ground. Afterwards the fuel velocity was gradually increased until liftoff was achieved. The blowout velocity was measured by increasing the jet velocity until the flame approached a meta-stable position, at which the trailing diffusion flame disappears, and the fuel velocity was increased at an incremental pace.



### **3.) Results and Discussion**

For this experiment, six different angles were chosen: 20°, 30°, 40°, 50°, 60°, and 70°. The 10° and 80° angles were not chosen due to their closeness to the 0° (coflow) and 90° (crossflow) orientations. At each angle, liftoff and blowout jet velocities were measured under four ambient flow velocities: 0 (still air), 0.25, 0.4, and 0.6 m/s. (Note: the velocity of 0.25 was chosen due to physical limitations of the blower motor.) Thus, twenty-four flow configurations are established. Table 1 contains the raw data collected for each configuration, along with the calculated values for liftoff and blowout velocity.

**Table 1. Liftoff and blowout velocities for all flow configurations.**

Parameters		Liftoff			Blowout		
Angle (°)	Coflow Velocity (m/s)	Meter Reading	Chart Value (ft <sup>3</sup> /h)	Liftoff Velocity (m/s)	Meter Reading	Chart Value (ft <sup>3</sup> /h)	Blowout Velocity (m/s)
20	0.00	43	29.9	17.22	147	123.2	70.96
20	0.25	42	29.2	16.82	140	115.8	66.70
20	0.40	37	25.5	14.69	136	111.8	64.39
20	0.60	32	21.7	12.50	131	107.2	61.74
30	0.00	46	32.2	18.55	145	121.0	69.69
30	0.25	43	29.9	17.22	143	118.9	68.48
30	0.40	40	27.7	15.95	143	118.9	68.48
30	0.60	35	24.0	13.82	139	114.8	66.12
40	0.00	47	33.0	19.01	147	123.2	70.96
40	0.25	42	29.2	16.82	138	113.8	65.54
40	0.40	36	24.7	14.23	137	112.8	64.97
40	0.60	32	21.7	12.50	132	108.1	62.26
50	0.00	47	33.0	19.01	145	121.0	69.69
50	0.25	44	30.7	17.68	148	124.3	71.59
50	0.40	40	27.7	15.95	148	124.3	71.59
50	0.60	33	22.5	12.96	143	118.9	68.48
60	0.00	51	36.2	20.85	150	126.4	72.80
60	0.25	46	32.2	18.55	147	123.2	70.96

60	0.40	47	33.0	19.01	150	126.4	72.80
60	0.60	37	25.5	14.69	150	126.4	72.80
70	0.00	46	32.2	18.55	150	126.4	72.80
70	0.25	47	33.0	19.01	148	124.3	71.59
70	0.40	45	31.5	18.14	143	118.9	68.48
70	0.60	36	24.7	14.23	150	126.4	72.80

As shown by Table 1, the jet velocity is much higher than that of the coflow, ensuring that all flames are jet flames, rather than wake-stabilized flames. For the highest coflow velocity, and the lowest jet velocity, at 20° with a jet velocity of 12.5 m/s and a coflow of 0.60 m/s, the jet to wind momentum flux ratio (R), which compares the momentum of the fuel jet to that of the ambient wind, was calculated to be 241.47, well above R=10 needed to define the jet as a strong jet, from Huang and Wang [16].

As expected, the flame shape varied with the angle, with the flame front conforming to the direction of the coflow. The photographs in Fig. 3 depict a flame at a 20° (less oblique) angle, as well as at 50° and 70° angles with a coflow velocity of 0.4 m/s. Three states are shown: the attached flame, the lifted flame, and the hysteresis flame just prior to blowout.



**Figure 3. Flame states at 0.4 m/s coflow.**

The overall data from Table 1 can be used to form a general stability chart based on the angle between the burner nozzle and coflow air, as shown in Fig. 4. Similarly, The data can be consolidated into a general chart based on coflow velocity, as shown in Fig. 5.

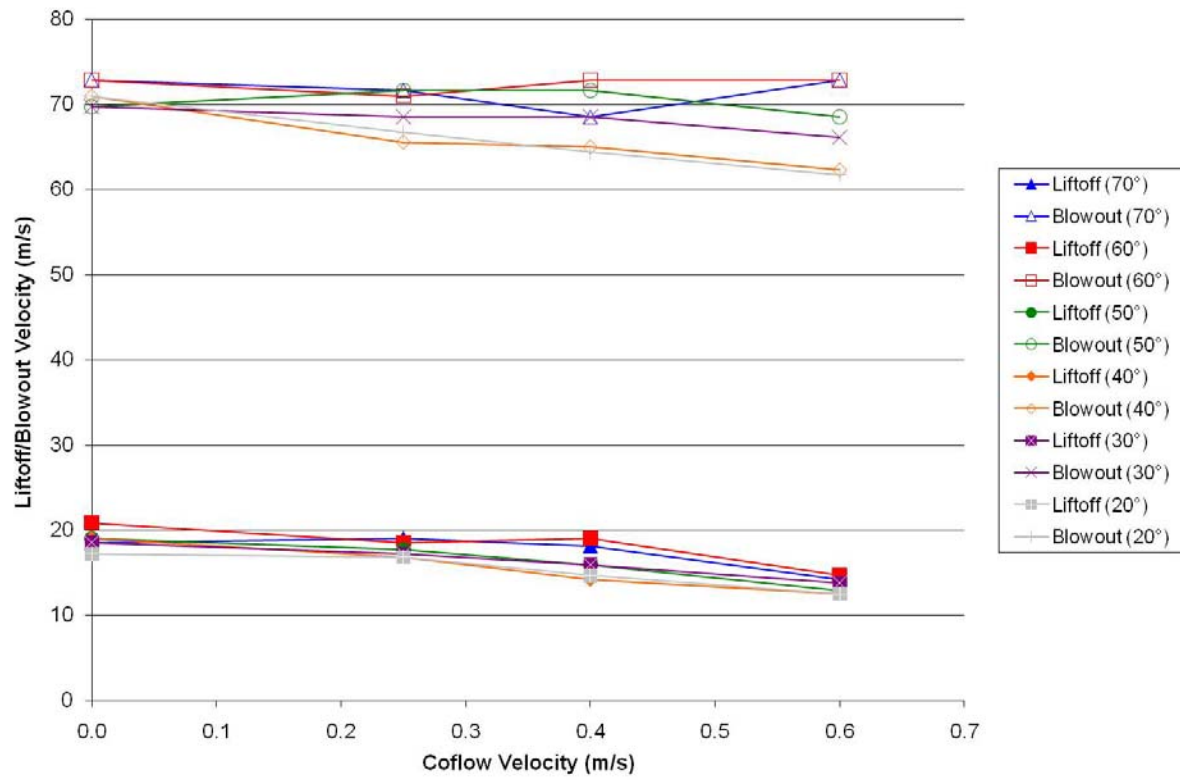


**Figure 4: Stability limits vs. coflow velocity for all angles.**

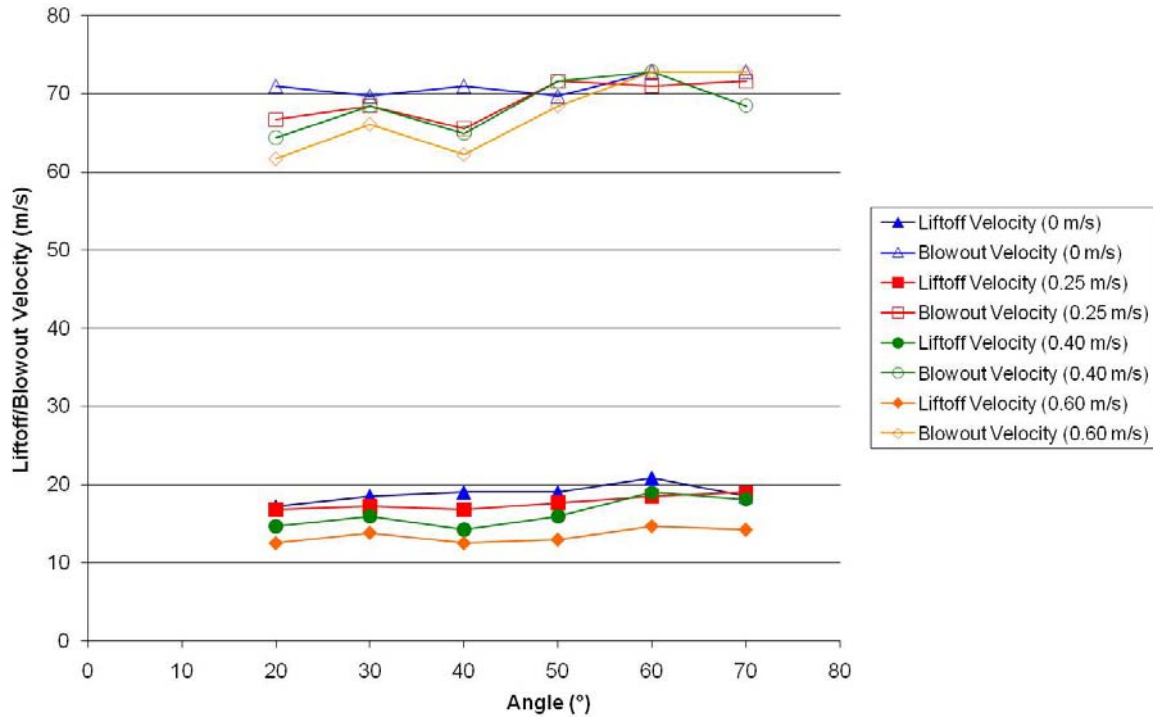


**Figure 5: Stability limits vs. angle for all coflow velocities.**

Based on Fig. 4, it can be seen that the flame liftoff velocity is largely resistant to changes in the nozzle angle. The greatest deviation occurs at a coflow velocity of 0.4 m/s. At each angle, liftoff velocity generally decreases with greater coflow velocity. This behavior can be attributed to the component of the coflow velocity vector that lies parallel to the flame direction. Thus, at greater coflow velocities, a lower fuel supply speed (liftoff velocity) is required for the flame to detach from the burner.

In contrast, the blowout velocities in Fig. 4 exhibit greater deviation with increasing coflow velocities. The nozzle angle has a more pronounced effect on blowout velocity under high coflow velocities—namely at 0.40 and 0.60 m/s. Figure 4 suggests that the blowout velocity increases for higher angles. For the 60° and 70° angles, the blowout velocity is over 70 m/s; however, for the 40°, 30°, and 20° angles, the blowout velocity is between 60-65 m/s. Since the

nozzle angle has a minimal effect on the liftoff velocity, it can be concluded that flames have a greater upper stability limit (blowout threshold) at more oblique nozzle angles, namely 60° and 70°.

The data in Fig. 5 exhibits behavior that conforms to the trends shown in Fig. 4. Again, it can be observed that liftoff velocity generally decreases under higher coflow velocities for the full range of nozzle angles (but with slightly less deviation at 70°). The blowout velocities demonstrate much more variation at smaller angles, with the greatest deviations at 20° and 40°. However, at 50°, 60°, and 70°, the blowout velocities show relatively less deviation. This result indicates that the nozzle angle has a stronger effect on blowout velocity than the coflow velocity, thus following the behavior shown in Fig. 4.

Overall, it can be concluded that flames at more oblique angles (50°-70°) have a greater upper stability limit that is also more resistant to changes in coflow velocity. This behavior is due to a reduced coflow velocity component that approaches zero as the nozzle angle approaches 90°. The effective coflow velocity is the component of the overall coflow velocity vector that lies along the flame/nozzle direction. With the coflow remaining vertical, this component diminishes as the nozzle angle increases towards the horizontal—that is, less of the coflow blows along the flame and contributes to liftoff/blowout behavior. The effective coflow velocity follows the equation below, as presented originally by Kalghatgi and recently by Moore et al [11] [17]. The effective velocity depends on the fuel and air densities, as well as the ambient and coflow velocities:

$$U_{eff} = U_0 + C\sqrt{\rho_{cf}/\rho_0}U_{cf}$$

Lastly, the relationship between the liftoff and blowout velocities under different flow configurations can be examined. The two stability limits can be plotted against each other, as

shown in Fig. 6 (ignoring coflow velocity). To determine the effect of nozzle angle on the flame stability limit ratio, non-dimensional analysis can be applied to the liftoff and blowout velocities. For each flow configuration, the coflow velocity is divided by the liftoff and blowout velocities to produce a dimensionless ratio. Therefore, the liftoff velocity ratio is equal to  $\frac{v_{coflow}}{v_{jet,liftoff}}$  and the blowout velocity ratio is  $\frac{v_{coflow}}{v_{jet,blowout}}$ . These ratios were derived the fact that the coflow velocity was limited to discrete levels, whereas the jet velocity varied. Figure 8 shows the liftoff and blowout velocity ratios plotted against each other. A strong linear relationship exists, suggesting that these two values remain in proportion to each other regardless of coflow velocity and angle.

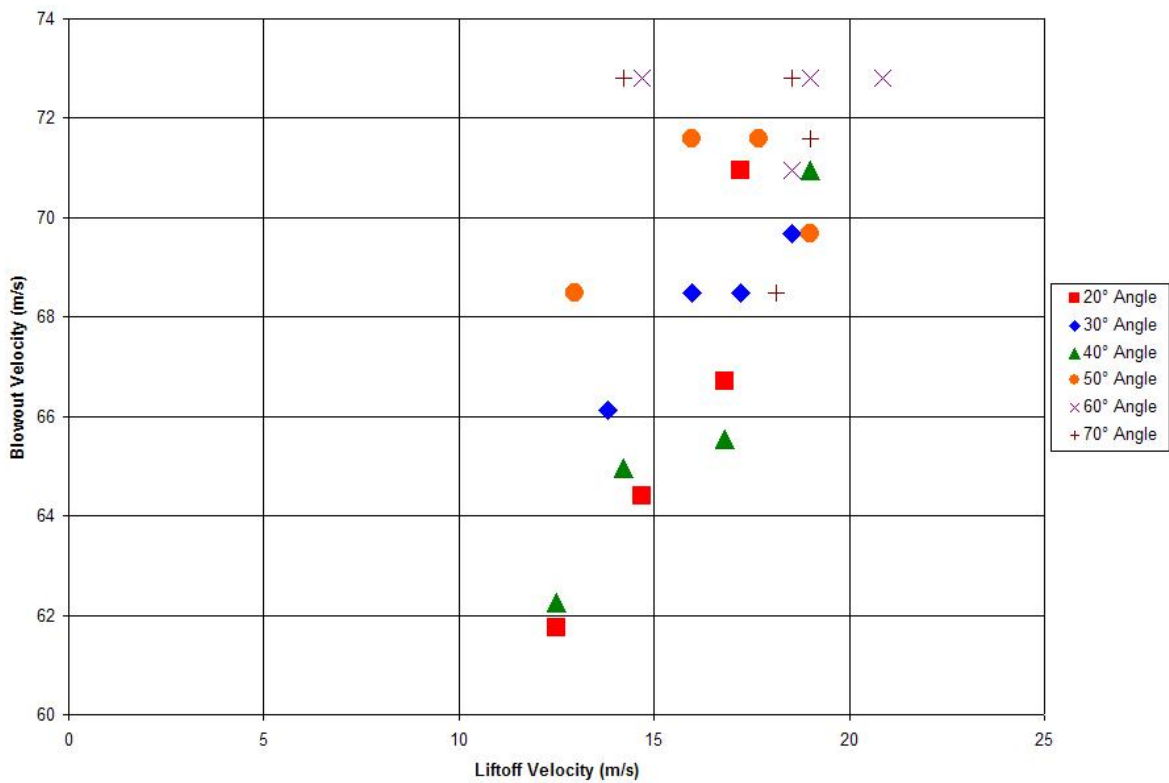


**Figure 6. Blowout velocity vs. liftoff velocity.**



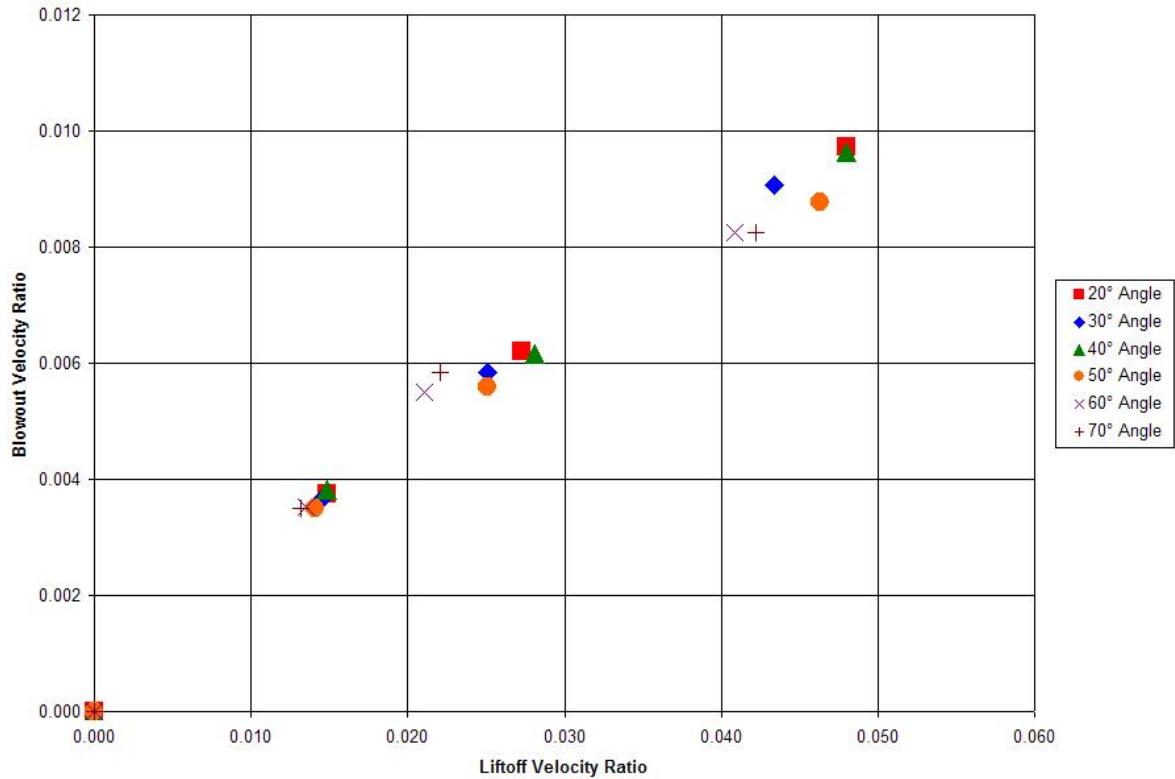


**Figure 7. Blowout velocity ratio vs. liftoff velocity ratio.**

As the results of Figs. 4 suggest, there is not a strong correlation between the liftoff velocity (lower stability limit) and flame angle. However, the angle seems to have an effect on the blowout velocity (upper stability limit) under high coflow velocities. Figure 6 supports this notion; showing generally lower values for both liftoff and blowout velocities for higher coflow velocities. For the liftoff velocity, the effect is uniform throughout all angles. However, for the blowout velocity, the effect is more pronounced at smaller angles, namely from 20° to 40°. The most deviation occurs at these points.

To gain further insight, liftoff and blowout velocities are determined for flames at 90° (crossflow) and 110° (mild counterflow). As with the previous angles, four coflow velocities are used, resulting in eight additional flow configurations. Table 2 contains the data obtained for these configurations, as well as calculated values for the liftoff and blowout velocities. Also, Fig.

8 shows the crossflow and counterflow flames in their three main states: attached, lifted, and pre-blowout hysteresis.

**Table 2. Liftoff and blowout velocities for 90° and 110° flow configurations.**

Parameters		Liftoff			Blowout		
Angle (°)	Coflow Velocity (m/s)	Meter Reading	Chart Value (ft <sup>3</sup> /h)	Liftoff Velocity (m/s)	Meter Reading	Chart Value (ft <sup>3</sup> /h)	Blowout Velocity (m/s)
90	0.00	48	33.8	19.47	150	126.4	72.80
90	0.25	46	32.2	18.55	150	126.4	72.80
90	0.40	47	33.0	19.01	150	126.4	72.80
90	0.60	43	29.9	17.22	150	126.4	72.80
110	0.00	54	38.6	22.23	150	126.4	72.80
110	0.25	55	39.4	22.69	150	126.4	72.80
110	0.40	57	41.0	23.61	150	126.4	72.80
110	0.60	57	41.0	23.61	150	126.4	72.80

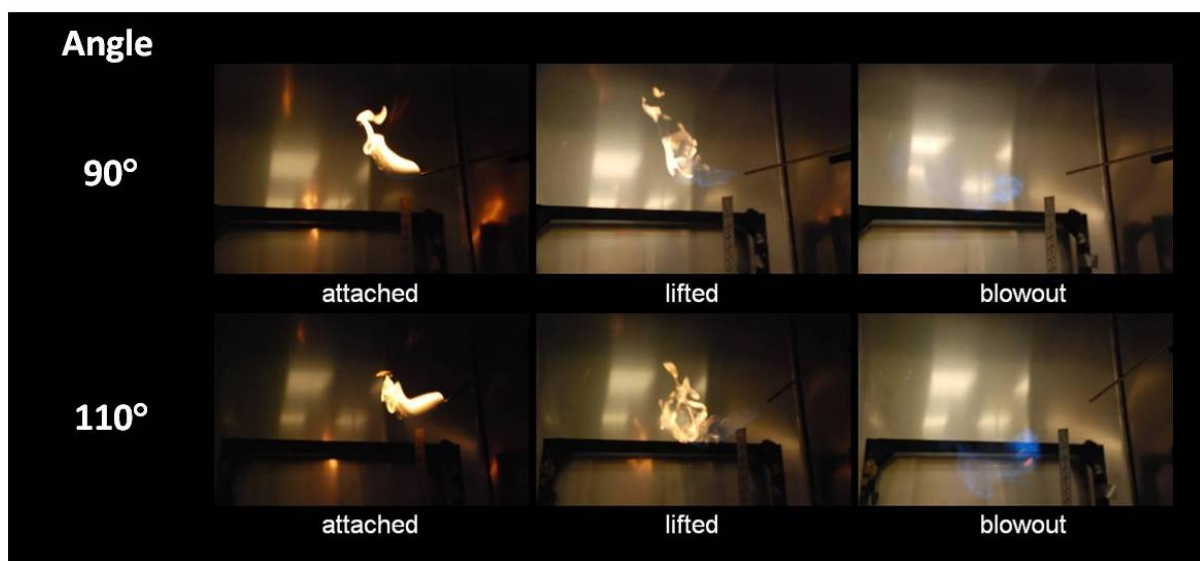


**Figure 8. Flame states at high oblique angles.**

Compared with the original data in Table 1, the liftoff and blowout velocities at  $90^\circ$  and  $110^\circ$  are greater than those for oblique angles from  $20^\circ$  to  $70^\circ$ . These velocities can be plotted against the original data as shown in Figs. 9 and 10.

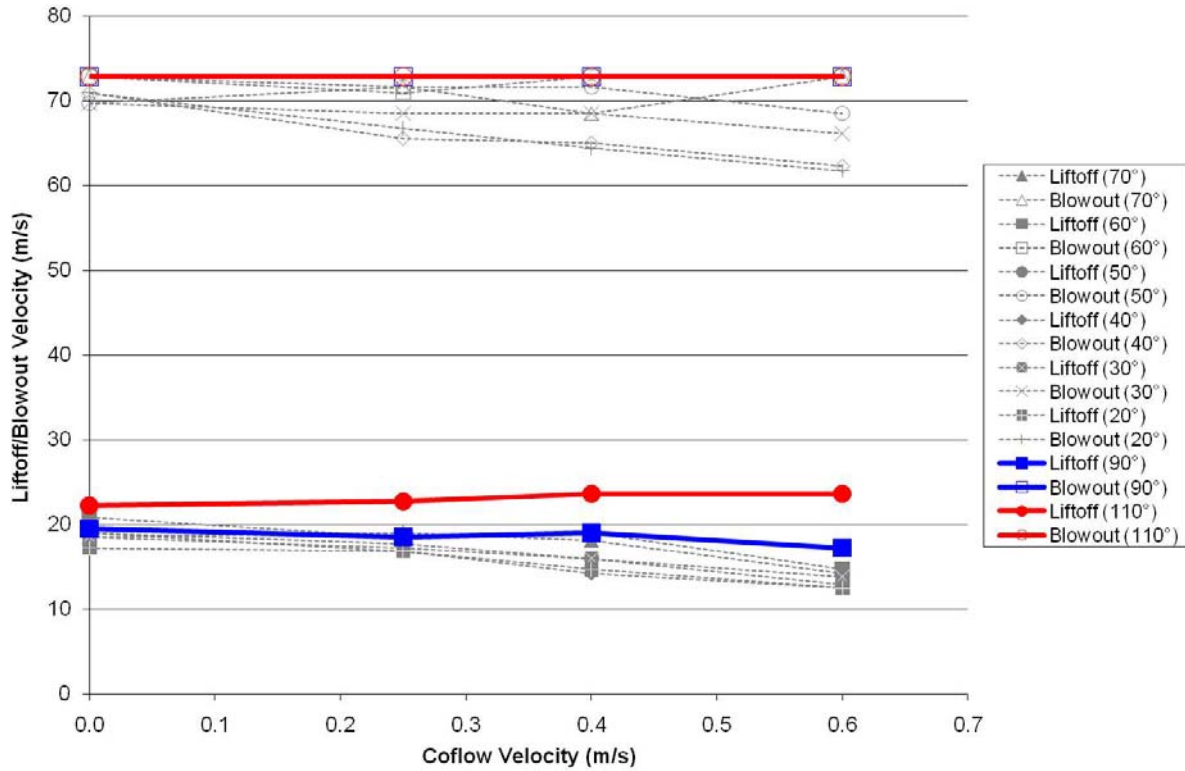


**Figure 9. Stability limits vs. coflow velocity including  $90^\circ$  and  $110^\circ$ .**

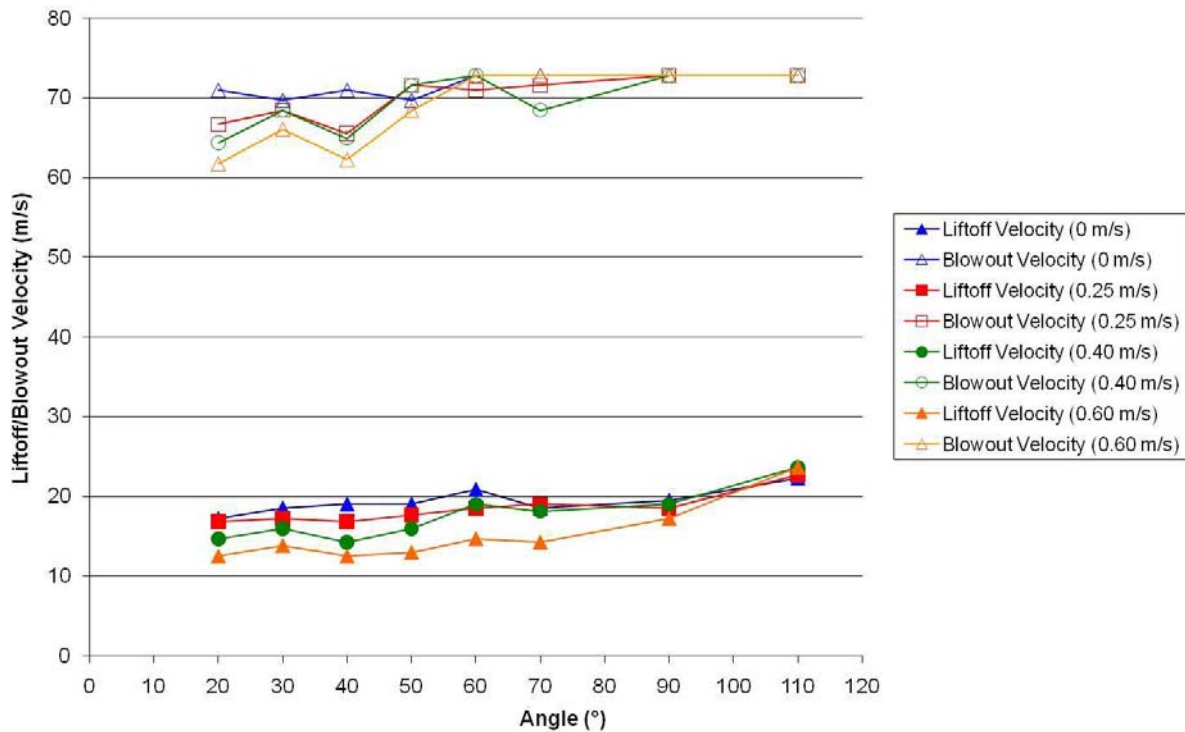


**Figure 10. Stability limits vs. angle including 90° and 110°.**

Note that the blowout velocity in Fig. 9 is a constant 72.80 m/s for all eight flow configurations. This limitation occurred due to high fuel flow rates that were beyond the indicating range of the flowmeter used in this experiment. Thus, the actual blowout velocity is beyond the 72.80 m/s reading used in Table 2 and Fig. 9. Regardless, this value is still sufficient in showing that the flame upper stability limit is generally higher for the 90° and 110° nozzle angles. Though the blowout velocity data is indeterminate, the liftoff velocities vary to a minimal degree with changing coflow velocities. Thus, the lower stability limit of flames in crossflow and mild counterflow is largely unaffected by coflow velocity.

Regarding Fig. 1, the lower stability limit (liftoff velocity) deviates much less for the 90° and 110° nozzle angles. This result also indicates that coflow velocity has an inconsequential effect on crossflow and mild counterflow flames. There is an overall increase—notably at the 110° nozzle angle—suggesting better stability behavior. (Again, in this case the blowout

velocities remain at a maximum of 72.80 m/s due to the limitations of the flowmeter used; the true blowout velocity is greater than this value.)

Previously, it was shown that flames at high oblique angles ( $50^{\circ}$ - $70^{\circ}$ ) have higher blowout velocities that are not affected much by coflow velocity. This conclusion applies to an even greater degree for the liftoff velocities of flames at  $90^{\circ}$  and  $110^{\circ}$  angles, which are higher and remain nearly constant regardless of coflow velocity. Though changes in blowout velocity could not be determined, the actual values exceed the velocities for oblique flames in the  $20^{\circ}$ - $70^{\circ}$  range. Thus, flames in crossflow and mild counterflow have higher stability limits than those in an oblique configuration.

#### 4.) Conclusions

Based on the results obtained from this experiment, a number of conclusions may be drawn regarding the stability of oblique jet flames in coflow:

1) Flame liftoff velocity is largely unaffected by the nozzle angle. However, the liftoff velocity generally decreases with increasing coflow velocity. This phenomenon is due to the coflow air contributing to the lifting of the flame, which results in a lower required fuel supply velocity (i.e., liftoff velocity).

2) Flames at more oblique angles ( $50^{\circ}$ - $70^{\circ}$ ) have a greater blowout velocity that is also more resistant to changes in coflow velocity. This behavior is due to a reduced effective coflow velocity that occurs at these angles. Overall, flames in these configurations are the most consistent in terms of upper and lower stability limits.

3) A strong linear relationship exists between the non-dimensional liftoff and blowout velocity ratios, which incorporate the coflow velocity. Thus, the actual liftoff and blowout velocities remain proportional to each other regardless of the coflow velocity and angle.

4) The blowout behavior for flames in crossflow ( $90^{\circ}$ ) and mild counterflow ( $110^{\circ}$ ) cannot be determined from the data obtained. However, the same data shows that the liftoff velocity of flames in crossflow and mild counterflow is largely unaffected by coflow velocity. In general, the lower stability limits (liftoff velocities) are higher than those for oblique flames in the  $20^{\circ}$ - $70^{\circ}$  range.

This experiment served as a basic observation of how the angle between a jet flame and its surrounding flow can affect the flame stability limits. A more extensive study would be required in order to fully understand the relation between these two factors. With more measurements at different ambient flow velocities, it may be possible for a mathematical model

to be developed (perhaps based on the previous work of Kalghatgi). A stronger correlation may exist under flow configurations not used in this experiment. Higher coflow velocities may be achieved with the use of a wind tunnel.

The data obtained revealed that an oblique flame in counterflow (i.e., at  $110^\circ$ ) behaves differently than an oblique flame in coflow (between  $0^\circ$  and  $90^\circ$ ). Further experiments can be performed to study flames at more extreme angles, such as those between  $90^\circ$  and  $180^\circ$ . Such work would help determine if counterflow flames can be utilized in efficient burner designs. Horizontal coflow orientations may also be investigated.

Additionally, this experiment only considered methane as the fuel source. Future experiments may be performed with propane, ethylene, hydrogen, or other commonly-used hydrocarbon fuel sources. Non-reacting diluents such as nitrogen can also be introduced in the fuel. Furthermore, the stabilizing effect of high coflow temperatures can be studied [18]. The equivalence ratio may be introduced as yet another parameter that can influence flame stability.

## REFERENCES

- [1] K. K. Kuo, *Principles of Combustion*, 2<sup>nd</sup> ed. New York: Wiley-Interscience, 2005.
- [2] K. Wohl, N.M. Kapp, and C. Gazley, "The Stability of Open Flames," *Third Symp. on Combustion and Flame, and Explosion Phenomena*, The Williams and Wilkins Company, pp. 3-21, 1949.
- [3] L. Vanquickenbourne and A. van Tiggelen, "The stabilization mechanism of lifted diffusion flames," *Combustion and Flame*, 10, pp. 59-69, 1966.
- [4] G.T. Kalghatgi, "Lift-off Heights and Visible Lengths of Vertical Turbulent Jet Diffusion Flames in Still Air," *Combustion Sci. and Tech.*, vol. 41, pp. 17-29, 1984.

- [5] C. D. Brown, K. A. Watson, and K. M. Lyons, "Studies on Lifted Jet Flames in Coflow: The Stabilization Mechanism in the Near- and Far-Fields," *Flow Turbulence and Combustion*, vol. 62, pp. 249-273, 1999.
- [6] S. R. Tieszen, D.W. Stamps, and T.J. O'Hern, "A Heuristic Model of Turbulent Mixing Applied to Blowout of Turbulent Jet Diffusion Flames," *Combustion and Flame*, vol. 106, pp. 442-466, 1996.
- [7] C.P. Burgess and C.J. Lawn, "The Premixture Model of Turbulent Burning to Describe Lifted Jet Flames," *Combustion and Flame*, vol. 119, pp. 95-108, 1999.
- [8] S. Navarro-Martinez and A. Kronenburg, "Analysis of Stabilization Mechanisms in Lifted Flames", *LES and DNS of Ignition Processes and Complex-Structure Flames with Local Extinction*, AIP Conf. Proceedings, vol. 1190, pp. 13-38, 2008.
- [9] R. V. Bandaru and S. R. Turns, "Turbulent Jet Flames in a Crossflow: Effects of Some Jet, Crossflow, and Pilot-Flame Parameters on Emissions", *Combustion and Flame*, vol. 121, pp. 137-151, 2000.
- [10] G.T. Kalghatgi, "Blow-Out Stability of Gaseous Jet Diffusion Flames Part II: Effect of Cross Wind", *Combustion Sci. and Tech.*, vol. 26, pp. 241-244, 1981.
- [11] G. T. Kalghatgi, "Blow-Out Stability of Gaseous Jet Diffusion Flames Part III: Effect of Burner Orientation to Wind Direction", *Combustion Sci. and Tech.*, vol. 28, pp. 241-245, 1982.
- [12] D. Han and M.G. Mungal, "Simultaneous measurements of velocity and CH distribution, part 2: deflected jet flames," *Combustion and Flame*, vol. 33, pp. 1-17, 2003.
- [13] E.F. Hasselbrink and M.G. Mungal, "Transverse jets and jet flames, part 2: Velocity and OH Field Imaging," *J. of Fluid Mechanics*, vol. 443, pp. 27-68, 2001.
- [14] J. L. McCraw, "Observations on Upstream Flame Propagation in Ignited Hydrocarbon Jets," M.S. thesis, Dept. Mech. and Aero. Eng., NC State Univ., Raleigh, NC, 2006.
- [15] S. D. Terry and K. M. Lyons, "Low Reynolds Number Turbulent Lifted Flames in High Co-Flow," *Combustion Sci. and Tech.*, vol. 177, pp. 2091-2112, 2005.
- [16] R.F. Huang and S.M. Wang, "Characteristic Flow Modes of Wake-Stabilized Jet Flames in a Traverse Air Stream," *Combustion and Flame*, vol. 117, pp.59-77, 1999
- [17] N. J. Moore, J. D. Kribs, and K. M. Lyons, "Investigation of Jet-Flame Blowout with Lean-Limit Considerations," *Flow, Turbulence and Combustion.*, vol. 87, pp. 525-536, 2011.
- [18] S. Lamige et al, "Effect of Reactant Preheating on the Stability of Non-Premixed Methane/Air Flames," in *Proc. Int. Heat Transfer Conf.*, Washington, D.C., 2010



## **Part B) Advances in Investigation of Jet-Flame Blowout with Lean-Limit Considerations**

### **Abstract**

The current study utilizes digital image sequences of flames to better understand the blowout phenomenon. Methane flames are studied near blowout conditions to determine if the disappearance of the diffusion flame prior to extinguishment signifies the leading edge of the reaction zone reaching the lean-limit. Various concentrations of nitrogen are used to dilute methane flames. The axial position of the flames is compared with the calculated position of the lean flammability limit to determine the role of the diffusion flame. The blowout limits of these flames are established and a blowout parameter is empirically determined from the data. Results from flames in co-flow show agreement with the blowout parameter previously published; however, the analysis shows that, the disappearance of the bulk diffusive reaction zone occurs at the lean flammability limit and is an accurate predictor of blowout for diluted and non-diluted methane flames.

### **Introduction**

Blowout is the result of a flame being unable to sustain combustion in general at positions far downstream from the burner exit. The flame arrives at this location due to high flow velocities that causes the reaction zone to recede to a position where it can stabilize. The reaction zone exists within the flammability limits of the fuel, and so when the concentration of fuel is too low, the flame blows out. The mechanisms that cause extinguishment are not fully understood and research continues in order to determine the processes involved in destabilization and blowout of a lifted jet flame.

Previously, experiments with methane flames in co-flowing air have shown that the disappearance of the diffusion flame is a visual predictor of blowout (Moore *et al.*, 2008). Analysis determined that the disappearance corresponded to the estimated location downstream of the lean limit contour. However, the findings of Moore *et al.* (2008) revealed that further investigation into the relationship between the flame position and the lean flammability limit is necessary because the estimate of the scalar field based on Tieszen's relation (Tieszen *et al.*, 1996) does not account for the presence of co-flow, and analysis is limited.

The effect of diluents on blowout has been studied in multiple configurations. Karbasi and Wierzbza (1998) examined blowout velocities for flames in which the fuel jet contained diluents, and cases in which the co-flowing stream contained a diluent. The conclusion was made that the presence of the diluent in the coflow has a greater influence on the blowout limit, compared to the case with the diluent is added within the jet. Dahm and Mayman (1990) experimented with methane and ethylene diluted with carbon dioxide or air. They devised a "flip" experiment in which the separate fuel and diluent streams could be switched such that either could issue from the center nozzle and the other from a surrounding nozzle. Their results showed that the blowout velocities from both configurations were almost equal, demonstrating that the blowout behavior is determined by mixing that occurs in the far-field. In experiments by Schefer and Baillot (1994), CH-PLIF (Planar Laser Induced Fluorescence) images were taken of methane jet flames, leading to the conclusion that the width of the flammable region is dependent on the vortical mixing structure. In further experiments by Wyzgolik *et al.* (2008), on methane jets in coflow, it was found that streamwise vortices are central to the stabilization of the flame.

Additionally, the velocities of methane, nitrogen and co-flowing air at blowout have been studied to determine a predictive parameter for various cases. Multiple studies have attempted to quantify blowout limits using a model based on fuel properties and a relation for the flow exit velocity (Broadwell *et al.*, 1984; Kalghatgi, 1981; Dahm and Dibble, 1988). This method of predicting blowout is highly reliant on the method by which the velocity of the fuel, diluent, or co-flow is measured. For example, the velocities in the far field can be characterized by the bulk jet exit velocity or by estimates of the flow field near the flame front. Generally, the blowout parameter decreases with increasing flow velocity such that a lower limit is established at which stable flames can exist. Analysis of this model is applied to the current research to describe the physical reasons for the blowout velocities recorded.

The current paper describes analysis performed on data obtained from experiments with nitrogen-diluted methane flames near blowout. Multiple fuel concentrations are tested after blowout flow velocities are determined for each set of conditions. Video images of the blowout process capture the flame prior to blowout, and assure the conditions are as repeatable as possible (for a somewhat unpredictable phenomenon like blowout). The results assist in determining if the disappearance of the diffusion flame consistently observed, prior to blowout, is directly related to the value of the local mixture fraction. A blowout parameter for these flames is also calculated, and a discussion of this method is provided with respect to data in the literature.

## **Experimental Procedure**

Experiments were performed with diluted methane flames at blowout conditions at Applied Energy Research Laboratory of North Carolina State University. Methane (99% pure) and nitrogen were directed through a fuel pipe of 3.5 mm (see Figure 1). The flow rate of the methane and the nitrogen were regulated with separate rotameters such that the amounts of methane and nitrogen issuing from the fuel pipe could be independently controlled. The length of the fuel pipe allows for the gases to fully mix before exiting. A butane lighter was used as the ignition source and was placed at the fuel pipe exit to ignite the jet after flow rates were set at the desired conditions. This burner was also used in a previous study to observe methane flames with co-flowing air (Moore *et al.*, 2008).

Blowout can be achieved by slowly increasing the jet exit velocity of a stable flame until the blowout velocity is reached. However, this method introduces error due to the inability to accurately record the changes in the flow rate at the jet exit. Wu *et al.* (2006) studied the changes in the stoichiometric contour at the flame front using acoustic excitation to control blowout in an easily repeatable procedure. Repeatability for the current study is achieved by keeping the flow rates constant and igniting the flame at the burner.

The flame was observed from ignition to blowout with recorded images obtained from a Panasonic Model PV-GS300 video camera. With an arbitrary rate of nitrogen chosen, the methane flow rate was adjusted until the flame was “meta-stable”. After several tests were made, the flow rate of methane necessary to cause the flame to blowout within approximately thirty seconds was determined, and these flow parameters then defined the meta-stable state. With the flow rate held to that blowout velocity, the jet was ignited at the pipe exit and the reaction zone observed to blowout multiple times. The recorded images of these flames were used to determine the height of the flame front at which the diffusion flame disappeared. The

flow rate of nitrogen was varied between 5.9 and 9.9 m/s and for each, several tests were used to determine the flow rate of methane to ensure blowout. No flame could be established with a nitrogen velocity greater than 9.9 m/s.

## Results and Discussion

Images of the flame from ignition to blowout are shown in Figure 2 for the case with methane velocity,  $U_{CH_4}$ , at 28.6 m/s and the nitrogen velocity,  $U_{N_2}$ , at 9.9 m/s (Table 1, bottom row, 37.6%  $N_2$ ). . Blowout occurred at 3 seconds after ignition at the burner. The diffusion flame is clearly witnessed until 2.83 seconds. The flame recedes quickly downstream to eventually blow out after the axially-oriented diffusion flame becomes invisible. Figure 3 shows images similarly obtained for  $U_{CH_4} = 49.6$  m/s and  $U_{N_2} = 8.1$  m/s (Table 1, third row, 22.2%  $N_2$ ). For this case, the diffusion flame disappears after 1.67 seconds and blowout occurs at 1.8 seconds. Extensive testing of flames at blowout reveal no trend in the time needed for a flame at blowout conditions to proceed from ignition to extinguishment (Moore *et al.*, 2008), however, the video images confirm that the fuel and diluents velocities create a situation where blowout is imminent (without the videos, the duration and repeatability of blowout events and metastable state lifetimes are unknown).

The height of the flame front at which the diffusion flame disappears has been hypothesized to occur at the lean limit of the fuel mixture. The flammability limits of fuels in air have been determined experimentally and are believed to be due to heat loss from the flame, flame stretch, and flame instabilities (Strehlow, 1984). The flammability limits for a mixture can

be calculated using Le Chatelier's principle, which is fairly accurate for mixtures containing hydrocarbons (Strehlow, 1984). The lean limit as a percent of volume,  $L$ , is calculated by

$$L_m = \frac{1}{\frac{x_1}{L_1} + \frac{x_2}{L_2} + \dots + \frac{x_J}{L_J}} \quad (1)$$

, where  $x$  is the mole fraction of the constitutive molecules (Weinberg, 1963). The lean flammability limit of methane is 5%, so the lean limit of a mixture of methane and nitrogen can be calculated from the volume fraction of methane by

$$L_m = \frac{1}{\frac{x_{CH_4}}{5.0} + 0} = \frac{5.0}{x_{CH_4}}, \quad (2)$$

assuming an ideal gas (Strehlow, 1984).

Table 1 provides the blowout velocities of methane and nitrogen, so called because a lower velocity of either gas would not produce a flame that blows out. It also gives the average height of diffusion flame disappearance for each case as observed from digital images. The highest and lowest heights correspond to the lowest and highest lean limits, respectively. The calculated lean limits for the five mixtures are shown in Table 1.

The time-averaged mass fraction of fuel,  $Y$ , into air with no co-flow present is

$$Y = 10 \cdot \left( \frac{\rho_0}{\rho_\infty} \right)^{1/2} \left( \frac{r_0}{z} \right) \exp \left\{ -57 \left( \frac{r}{z} \right)^2 \right\} \quad (3)$$

, where  $\rho_0$  is the density of the jet,  $\rho_\infty$  is the ambient density,  $r_0$  is the jet nozzle diameter,  $r$  is the radial location of the flame, and  $z$  is the axial location (Tieszen *et al.*, 1996). As Chen and Rodi

(1980) state, the constants in the equation are only valid for downstream similarity regions where the density ratio is unity; however, a large change in density does not significantly change the behavior so the constants can be used for the entire downstream area. The similarity region begins at about twenty nozzle diameters downstream (Dowling and Dimotakis, 1990).

The scalar field established by Equation 3 accounts for dilution in the fuel stream. The density at the jet exit,  $\rho_0$ , is the density of the fuel mixture. The flow velocities of methane and nitrogen set by the rotameter of each were, along with the gas densities, used to determine the mass flow rate of each gas. The density of the mixture was then calculated by

$$\rho_0 = Y_{CH_4} \rho_{CH_4} + Y_{N_2} \rho_{N_2} \quad (4)$$

where the mass fraction,  $Y$  is determined by

$$Y_i = \frac{\dot{m}_i}{\dot{m}_i + \dot{m}_j} \quad (5)$$

for a mixture of  $i$  and  $j$  with the mass flow rate  $\dot{m}$ .

Figure 4 shows the graphical results of these experiments. For each fuel velocity, the height at which the diffusion flame disappears is plotted with the average of the data and the estimated height of the lean limit. In each case, the diffusion flame disappears within 3 cm of the lean flammability limit. This data supports the conclusion that during blowout the reaction zone at the flame front moves to a downstream location at which all fuel is burnt locally. Burning at the lean limit does not leave enough fuel-rich gases to support a diffusion flame. Blowout occurs quickly after the diffusion flame disappears and at a location slightly beyond the location of the lean limit.

Broadwell *et al.* (1984) defines a blowout criterion as the ratio between the mixing time and the chemical time. The molecular mixing between the fuel and entrained air is caused by inviscid motions scaled with the local jet diameter,  $\delta$ , and associated with time

$$t_m = \frac{\delta}{u} \quad (6)$$

where  $u$  is the local velocity. The fluctuations eventually reach the Kolmogorov scale. Diffusion at this scale is associated with time,  $t_\lambda$ ,

$$t_\lambda = \frac{\delta}{u} \left( \frac{Sc}{Re} \right)^{1/2} \quad (7)$$

where  $Sc$  is the Schmidt number and  $Re$  is the Reynolds number. At high Reynolds numbers like those seen at blowout, the small scale diffusion can be neglected and the mixing time is approximated as Equation 6. Thus, the critical parameter,  $\varepsilon$ , is

$$\varepsilon \equiv \frac{t_m}{t_c} \propto \frac{\delta / u}{\kappa / S_L^2} \quad (8)$$

which can be rewritten as

$$\varepsilon = \frac{d S_L^2 \psi^2 \left( \frac{\rho_0}{\rho_\infty} \right)^{1/2}}{u \kappa} . \quad (9)$$

Equation 9 uses conservation of momentum and similarity to put  $\varepsilon$  in terms of the fuel pipe diameter,  $d$ , and properties of the fuel (Broadwell *et al.*, 1984). Kalghatgi (1981) provides the values used by Broadwell *et al.* (1984):  $\psi$  (stoichiometric air to fuel ratio) = 17.2,  $S_L$  (laminar burning velocity) = 0.39 m/s, and  $\kappa$  (thermal diffusivity) =  $4.56 \times 10^{-4} \text{ m}^2/\text{s}$ .



The velocity in Equation 9 can be approximated as the jet exit velocity at blowout in order to determine the critical value of  $\varepsilon$  at blowout. Because the jet exit diameter was the same, it follows that a constant value of  $\varepsilon$  requires a constant  $u$ . Broadwell *et al.* (1984) found  $\varepsilon \approx 4.6$  for methane, and Dahm and Dibble (1988) found  $\varepsilon \approx 4.3$  for methane with co-flow. To calculate this parameter for the flames with co-flow analyzed in Moore *et al.* (2008), an effective velocity is used

$$U_{eff} = U_0 + C \sqrt{\rho_{cf} / \rho_0} U_{cf} \quad (10)$$

where  $C = 40$  (Kumar *et al.*, 2007), where all subscripts cf refer to characteristics of the coflow. Using this velocity gives a range of  $\varepsilon$  from 3.9 to 4.9 and an average  $\varepsilon$  of 4.35 a value in good agreement with the previous studies. Table 2 provides the data from these experiments and the effective velocities calculated, and Figure 5 plots the blowout velocities. For  $\varepsilon < 4.35$ , the flow velocities are such that blowout is predicted to occur.

Figure 6 shows that the relationship between the amount of methane and nitrogen in a blowout mixture is nonlinear, which is an obvious departure from the behavior of Figure 5. The dashed line delineates the fuel and nitrogen velocities that will result in blowout and those that will not. A flowrate of about 10 m/s or higher of nitrogen will most likely result in blowout. At high enough velocities of either gas, ignition may not result in anything but localized combustion.

The velocity of the fuel decreases linearly as the diluent concentration increases, as seen in Figure 7. The change in the diluent velocity however creates a parabola when plotted with the concentration. The combined velocity is the total jet exit velocity issuing from the fuel pipe.

Dahm and Mayman (1990) modified Equation 9 to correct for large diluent concentrations.

Thus,  $\psi$  is replaced by  $\phi$  where

$$\phi = (1 - Y_{N_2})\psi . \quad (11)$$

Equation 9 then becomes

$$\varepsilon = \frac{dS_L^2 (1 + \phi)^2 \left( \frac{\rho_0}{\rho_\infty} \right)^{1/2}}{u\kappa} . \quad (12)$$

As shown in Table 3, using the combined velocity in Equation 12 and the mixture density results in a range of  $\varepsilon$  from 3.4 to 4.0 and an average  $\varepsilon$  of 3.59. This value is slightly lower than that found by Weiland and Strakey (2009) of  $\varepsilon = 4.92$  for confined nitrogen-diluted hydrogen flames. The discrepancy can be due to differences in defining the velocity or in the gas properties used. The data shown in Figure 6 is consistent with studies of other diluted flames and this behavior provides insight into the blowout phenomenon.

## Conclusions

Further analysis of the blowout phenomenon has helped to verify the importance of the diffusion flame and establish a parameter for predicting blowout. Conclusions made from analysis of the diluted-methane flames and those of methane flames with co-flow are as follows:

1. Images obtained from experiments with diluted-methane flames indicate that the diffusion flame shortens and disappears as the flame proceeds towards blowout. Once the chemiluminescence of the diffusion flame is no longer observed, the existing flame front moves quickly downstream and blowout occurs rapidly.

2. Data from both flames with co-flow and diluted flames show that the calculation of the blowout criterion is highly dependent on the method used to determine the velocity of the jet mixture downstream. For diluted flames, this parameter is about 3.59. For flames with co-flow, it is about 4.3.
3. The parabolic relationship between the methane and nitrogen velocities results in the nitrogen concentration decreasing with increasing methane velocity. At the greatest nitrogen velocity, the concentration is 0.38. To achieve a higher concentration the rate of nitrogen must be decreased. This behavior is markedly different from flames of pure methane in the presence of co-flow where the velocities have a linear relationship. Dahm and Mayman (1990) also found a parabolic relationship between fuel and diluent velocities using air as the diluent. Thus, despite blowout occurring far downstream, it is affected by the mixing that occurs at the burner, since a jet of fuel/air has different blowout limits than a fuel jet surrounded by co-flowing air.

There exists (within the range where combustion is possible) two different fuel velocities at which blowout will occur for a given diluent velocity. Blowout is therefore not dependent on diluent concentration or on the amount of turbulence as defined by the Reynolds number (Broadwell *et al.*, 1984). The disappearance of the diffusion flame remains, however, a consistent indicator that blowout is imminent. Regardless of the diluent concentration, the disappearance occurs at the lean flammability limit.

## References

Broadwell, J.E., Dahm, W.J.A., and Mungal, M.G. Blowout of Turbulent Diffusion Flames. *Proceedings of the Combustion Institute*, The Combustion Institute, Pittsburgh, 20: 303-10, 1984.

Chen, C.J. and Rodi, W. Vertical Turbulent Buoyant Jets – A Review of Experimental Data, Pergamon, Oxford, 1980

Dahm, W.J.A. and Dibble, R.W. Co-Flowing Turbulent Jet Diffusion Flame Blowout. *Proceedings of the Combustion Institute*, The Combustion Institute, Pittsburgh, 22: 801-08, 1988.

Dahm, W.J.A. and Mayman, A.G. Blowout Limits of Turbulent Jet Diffusion Flames for Arbitrary Source Conditions. *AIAA Journal*, 28 (7): 1157-62, 1990.

Dowling, D.R. and Dimotakis, P.E. Similarity of the Concentration Field of Gas-Phase Turbulent Jets. *Journal of Fluid Mechanics*, 218: 109-141, 1990.

Kalghatgi, G.T. Blowout Stability of Gaseous Jet Diffusion Flames. Part 1: In Still Air. *Combustion Science and Technology*, 26: 233-39, 1981.

Karbasi, M. and Wierzbka, I. Prediction and Validation of Blowout Limits of Co-Flowing Jet Diffusion Flames – Effect of Dilution. *ASME Journal of Energy Resources Technology*, 120: 167-71, 1998.

Kumar, S., Paul, P.J., and Mukunda, H.S. Prediction of Flame Liftoff Height of Diffusion/Partially Premixed Jet Flames and Modeling of Mild Combustion Burners. *Combustion Science and Technology*, 179: 2219-53, 2007.

Moore, N., McCraw, J., and Lyons, K. Observations on Jet-Flame Blowout. *International Journal of Reacting Systems*, Article ID 461059, doi:10.1155/2008/461059, 2008.

Schefer, R.W. Namazian, M., and Kelly J. Stabilization of Lifted Turbulent-Jet Flames, *Combustion and Flame*. 99: 75-86, 1994.

Strehlow, Roger A. Combustion Fundamentals. McGraw-Hill, New York, 1984.

Tieszen, S.R., Stamps, D.W., and O'Hern, T.J. A Heuristic Model of Turbulent Mixing Applied to Blowout of Turbulent Jet Diffusion Flames, *Combustion and Flame*, 106: 442-66, 1996.

Weiland, N.T. and Strakey, P.A. Stability Characteristics of Turbulent Hydrogen Dilute Diffusion Flames. *Combustion Science and Technology*, 181: 756-81, 2009.

Weinberg, F.J. Optics of Flames. Butterworth & Co. (Publishers) Ltd., London, 1963.

Wu, C.-Y., Chao, Y.-C., Cheng, T.-S., Li, Y.-H., Lee, K.-Y., and Yuan T. The Blowout Mechanism of Turbulent Jet Diffusion Flames. *Combustion and Flame*, 145: 481-94, 2006.

Wyzgolik, A., and Baillot, F. Non-Premixed Lifted Flame Stabilization Coupled With Vortex Structures In a Coaxial Jet. *Combustion Science and Technology*, 180: 1956-71, 2008.

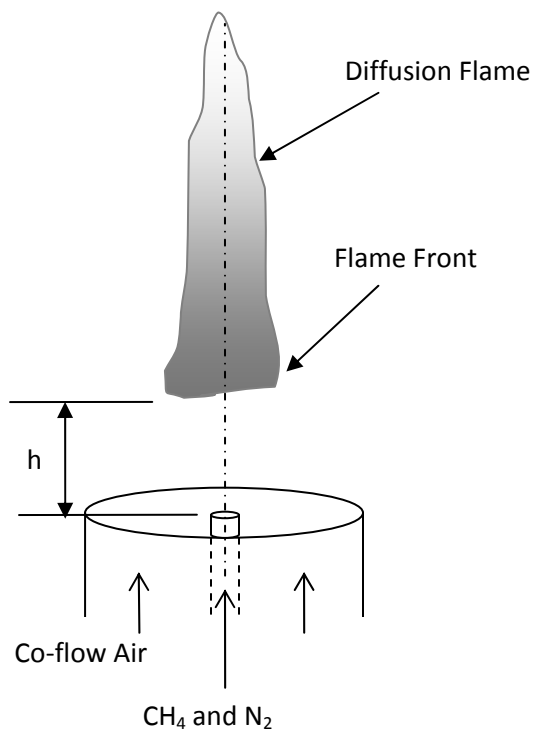


Figure 1. Vertical jet flame burner delivers methane and nitrogen through center pipe surrounded by co-flowing air.  $h$  is the axial height of the flame front from the burner.



(a)  $h = 10.7$  cm

$t = 0.73$  s



(b)  $h = 14.2$  cm

$t = 2.17$  s



(c)  $h = 19.1$  cm

$t = 2.77$  s



(d)  $h = 20.8$  cm

$t = 2.8$  s



(e)  $h = 22.7$  cm

$t = 2.83$  s



(f)  $h = 25.2$  cm

$t = 2.87$  s



(g)  $h = 27.4$  cm

$t = 2.9$  s



(h)  $h = 30.0$  cm

$t = 2.93$  s

Figure 2. Images of flame for  $U_{CH_4} = 28.6$  m/s,  $U_{N_2} = 9.9$  m/s.



(a)  $h = 8.8$  cm

$t = 0.37$  s



(b)  $h = 15.1$  cm

$t = 0.8$  s



(c)  $h = 13.9$  cm

$t = 1.27$  s



(d)  $h = 19.5$  cm

$t = 1.43$  s



(e)  $h = 23.2$  cm

$t = 1.6$  s



(f)  $h = 27.4$  cm

$t = 1.67$  s



(g)  $h = 31.3$  cm

$t = 1.7$  s



(h)  $h = 35.7$  cm

$t = 1.73$  s

Figure 3. Images of flame for  $U_{CH_4} = 49.6$  m/s,  $U_{N_2} = 8.1$  m/s.

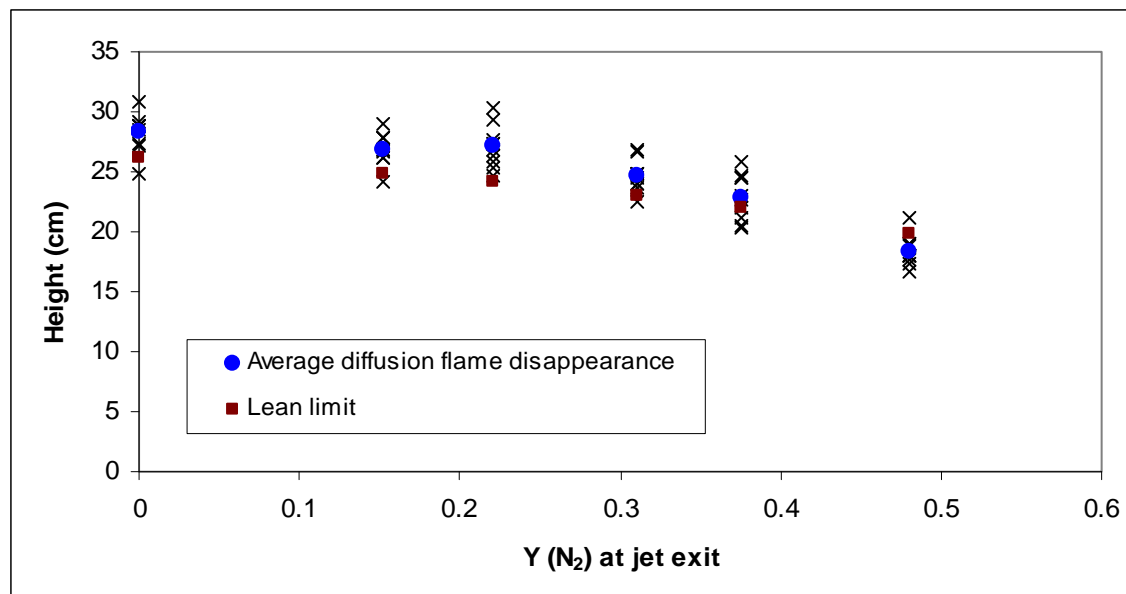


Figure 4. Height of the disappearance of the diffusion flame and the lean limit for each case (x) and the average.



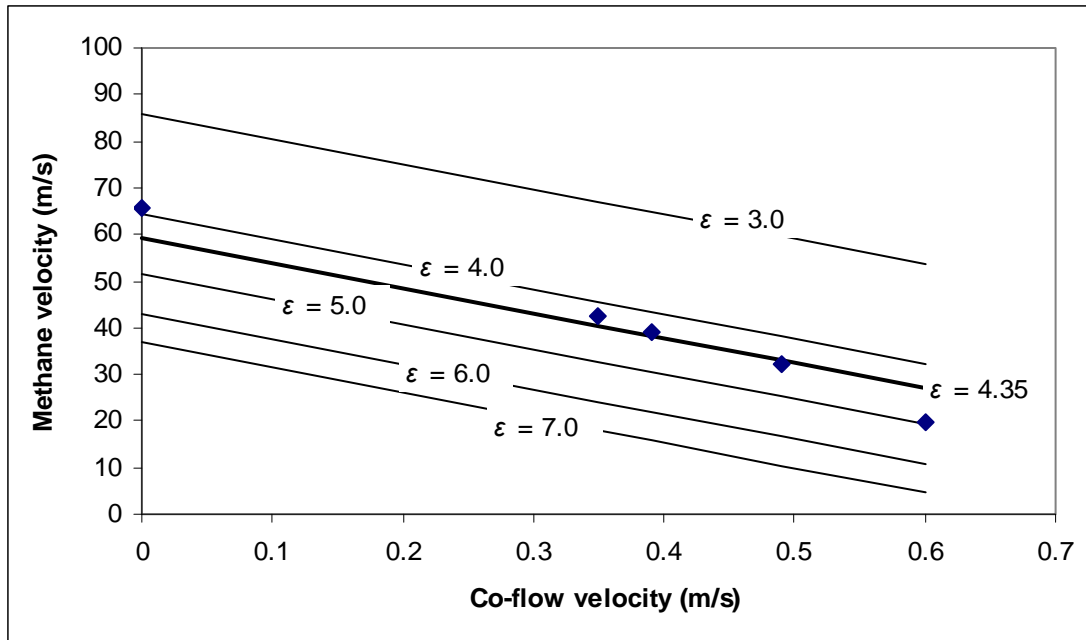


Figure 5. Velocities required for blowout shown with  $\varepsilon$  contours.

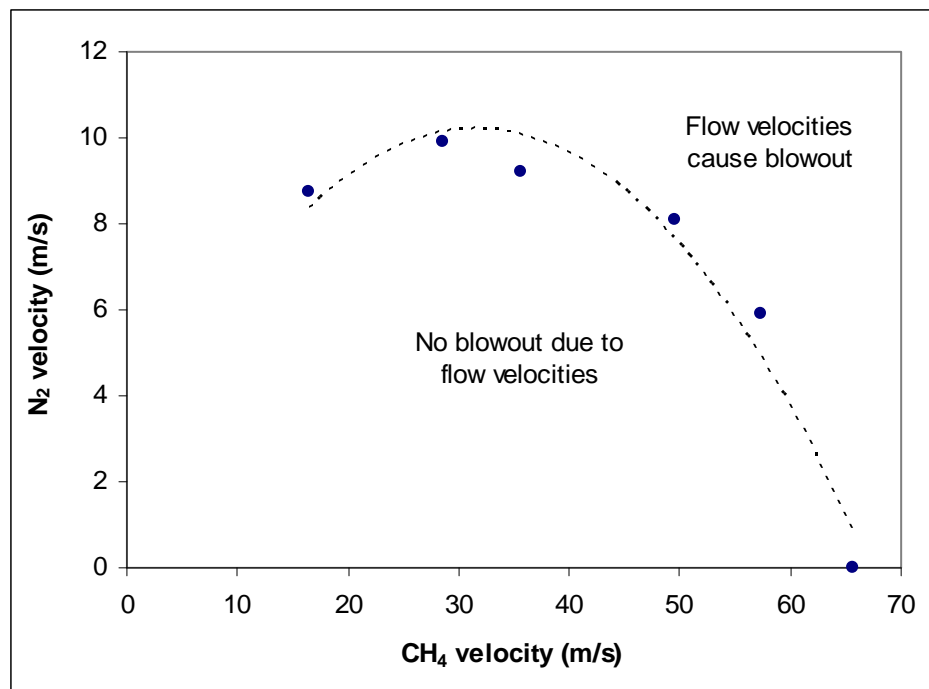


Figure 6. Methane and nitrogen velocities for flame blowout.

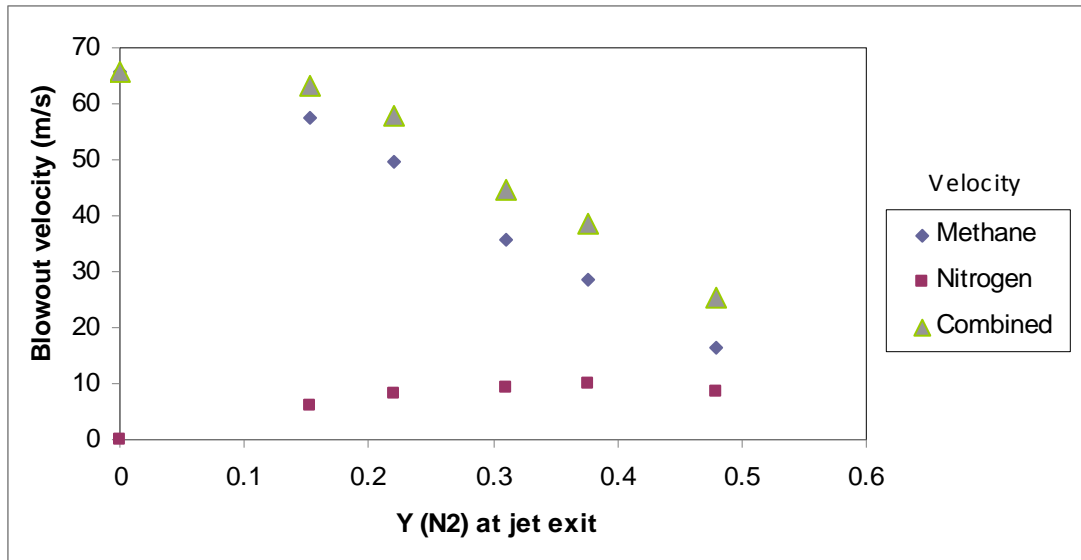


Figure 7. Flow velocities for each diluent concentration tested.

Nitrogen velocity (m/s)	Methane velocity (m/s)	Average height at diffusion flame disappearance (cm)	Lean flammability limit	Height of lean flammability limit (cm)
0.0	65.7	28.3	5.0 %	26.1
5.9	57.4	26.9	5.5%	24.9
8.1	49.6	27.1	5.8%	24.2
8.7	16.5	18.4	7.6%	19.9
9.2	35.6	24.7	6.3%	23.0
9.9	28.6	22.9	6.7%	22.0

Table 1. Flow rates of nitrogen and methane used to cause blowout.

Methane velocity (m/s)	Co-flow velocity (m/s)	$U_{eff}$ (m/s) – Equation 10	$\varepsilon$
65.7	0.0	65.7	3.9
42.4	0.35	61.2	4.2
39.0	0.39	59.9	4.3
32.2	0.49	58.5	4.4
19.6	0.6	51.8	4.9

Table 2. Blowout velocities for flames with co-flow.

Methane velocity (m/s)	Nitrogen velocity (m/s)	Combined velocity (m/s)	$\varepsilon$
57.4	5.9	63.3	3.5
49.6	8.1	57.7	3.4
35.6	9.2	44.8	3.6
28.6	9.9	38.5	3.5
16.5	8.7	25.3	4.0

Table 3. Blowout velocities for diluted flames.